Probing In-Flight Shell Breakup in DT Cryogenic Implosions on OMEGA

R. C. Shah,[1] S. X. Hu,[1] I. V. Igumenshchev,[1] J. Baltazar,[1] D. Cao,[1] C. J. Forrest,[1] V. N. Goncharov,[1] V. Gopalaswamy,[1] D. Patel,[1] F. Philippe,[2] W. Theobald,[1] and S. P. Regan[1]

[1]Laboratory for Laser Energetics, University of Rochester
[2]Commissariat à l'énergie atomique et aux énergies alternatives, France

On the 30-kJ OMEGA laser, experiments are conducted on spherical implosions to create conditions relevant to inertial confinement fusion. Plastic capsules (~1 mm in diameter) containing a cryogenic shell of solid hydrogen fuel are directly imploded by ~20 TW of laser power arriving via 60 beams. The dense shell acts as a piston to create a fusion-relevant pressure (~100 Gbar) and temperature (~3 to 5 keV) in DT plasma termed the "hot spot." The OMEGA experiments are interpreted by hydrodynamic scaling to the ~2-MJ National Ignition Facility for which the implosion dimensions would be large enough for hot-spot fusion reactions to cause runaway self-heating. Substantial progress has occurred[1] but the hot-spot conditions are not yet sufficient to trigger a self-sustained fusion reaction.[2]

Hot-spot performance is sensitive to the in-flight shell density ρ_{sh}, which, along with the shell velocity v_{sh}, determines the dynamic pressure of the imploding shell $P_d = \rho_{sh} v_{sh}^2$. The dynamic pressure determines the compressive work done to create the hot-spot pressure $P_{hs} \sim P_d^{5/3}$ (Ref. 3). A fundamental limit on the shell density arises from entropy, which is determined in direct-drive implosions mainly by laser pulse shape and resulting shocks. It is characterized by adiabat α defined as the ratio of the pressure to the Fermi-degenerate pressure at the shell density. However, the ablation surface is hydrodynamically unstable to perturbations,[4] and implosions having a higher adiabat tend to be more robust due to reduced instability growth rates and a lower-density, thicker shell. A dominant source of perturbations in direct-drive implosions is expected to be laser speckle or laser imprinting.[5–7]

The instability growth that breaks up the high-density shell leads to a relaxed density profile. A signature of the additional mass entering the hot-spot region is an increase of the early production of hot-spot soft x-ray emission. In this summary we interpret the onset of hot-spot x-ray self-emission from gated images of DT cryogenic implosions. Whereas the advance in onset of emission is well matched by imprint as calculated by the 3-D radiation-hydrodynamic code *ASTER*[8,9] for a low-adiabat implosion, this is not the case for more-stable, higher-adiabat implosions. The results suggest that other perturbations, not included in models, cause decompression of more-stable implosions.

We first consider three DT cryogenic implosions with α of 1.7, 3.0, and 5.5 (also referred herein as low-, mid-, and high-stability). For the highest-adiabat implosion the cryogenic layer was 30% thicker, thereby further augmenting its stability. The implosions were pinhole imaged at magnification $M = 6$ onto an x-ray framing camera and recorded on film with filtration to record soft (~800-eV) x rays. In these images the ablation front is identified with an outer emission limb. To quantify the advance of the turn-on, we have tracked the increase of the core emission as a function of ablation-front position. The relative core emission is calculated from each framed image as $2/\left(R_{pk}/2\right)^2 \int rI(r)\mathrm{d}r$, where $I(r)$ is the angle averaged signal normalized to the peak at the emission limb and R_{pk} is the peak position of the limb. These results are plotted for the low-, mid-, and high-stability implosions in Figs. 1(a)–1(c), respectively. The solid black circles and blue line correspond to the experimental measurements and fit; the dotted black line is the uniform *ASTER* calculation; and the dashed red line is the *ASTER* model including imprint. The data and simulation are fit using a delayed exponential with constant offset. A slight difference can be present in the offsets, which likely

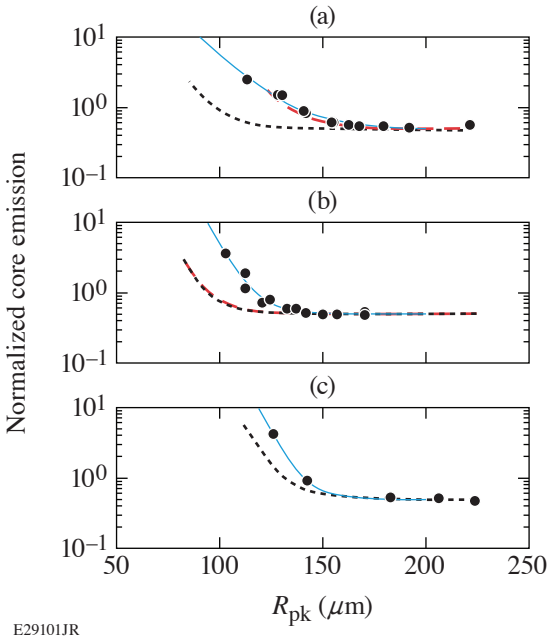

Figure 1
Central emission versus inferred ablation front radius for (a) low-, (b) mid-, and (c) high-stability implosions. Data are indicated by solid circles with blue line showing fit. Results from uniform *ASTER* are indicated by dotted black line for all three cases. High-resolution *ASTER* with laser imprinting is shown by dashed red line (low- and mid-stability cases only).

arises from inaccuracies in modeling the coronal plasma. To emphasize the emission turn-on, the fit offsets are subtracted and all curves are identically offset by the value obtained from the fit of the uniform model. The emission turn-on is then defined to occur at the normalized emission of unity. We find for the low-adiabat [Fig. 1(a)], this turn-on occurs at a radius 38.4±2 μm larger than what is determined by the identical analysis of the uniform *ASTER* calculation but is only slightly underpredicted with the *ASTER* model including imprint. From the *ASTER* model we find that the early onset of the emission is the result of mass jetting into the hot spot as a result of the instability growth. Figure 1(b) shows that a substantial discrepancy of 22.7 μm with the uniform calculation is present for the mid-adiabat, but that in this case the imprint results in no significant modification of the model. As shown in Fig. 1(c), the discrepancy with the uniform calculation is smallest for the most-stable implosion (such stable implosions show no impact from imprinting in calculations and therefore the 3-D high-resolution calculation was not conducted for this specific case). Several additional implosions were examined and supported the presence of a trend of reduced discrepancy in the emission onset with increased stability. In addition we also observed that for the most-stable implosion, the spatial profile of the emission for that implosion exhibited a flat (top-hat) profile of the core emission. Such a profile is observed in a 1-D calculation. The closer agreement of these characteristics for the 1-D prediction for the highly stabilized implosion suggests a role of unmodeled hydrodynamic perturbations in the cryogenic experiments.

In summary, time- and space-resolved characterization of the onset of core x-ray emission were used to diagnose conditions at the start of deceleration. With respect to understanding current limitations on hot-spot performance, the x-ray emission onset provides first evidence of good agreement with a 3-D radiation-hydrodynamic model of laser imprint in a low-adiabat, integrated DT cryogenic implosion. However, these measurements also suggest that additional perturbations beyond imprint remain to be identified and mitigated in the scaled direct-drive DT cryogenic implosions.

This material is based upon work supported by the Department of Energy National Nuclear Security Administration under Award Number DE-NA0003856, the University of Rochester, and the New York State Energy Research and Development Authority.

1. V. Gopalaswamy *et al.*, Nature **565**, 581 (2019).

2. R. Betti *et al.*, Phys. Rev. Lett. **114**, 255003 (2015).

3. V. N. Goncharov *et al*., Phys. Plasmas **21**, 056315 (2014).

4. S. Atzeni and J. Meyer-ter-Vehn, *The Physics of Inertial Fusion: Beam Plasma Interaction, Hydrodynamics, Hot Dense Matter*, 1st ed., International Series of Monographs on Physics, Vol. 125 (Oxford University Press, Oxford, 2004).

5. P. B. Radha *et al*., Phys. Plasmas **12**, 032702 (2005).

6. V. A. Smalyuk *et al*., Phys. Rev. Lett. **103**, 105001 (2009).

7. S. X. Hu *et al*., Phys. Rev. Lett. **108**, 195003 (2012).

8. D. T. Michel *et al*., High Power Laser Sci. Eng. **3**, e19 (2015).

9. I. V. Igumenshchev *et al*., Phys. Plasmas **23**, 052702 (2016).